

A Multi-UAV Coordination Scheme for Tracking Control of Multiple Moving Target Objects

Tua A. Tamba*

*Department of Electrical Engineering
Parahyangan Catholic University
Bandung, Indonesia
ttamba@unpar.ac.id*

Immanuel R. Santjoko

*Department of Electrical Engineering
Parahyangan Catholic University
Bandung, Indonesia
6152001008@student.unpar.ac.id*

Yul Y. Nazaruddin

*Department of Engineering Physics
Institut Teknologi Bandung
Bandung, Indonesia
yul@itb.ac.id*

Vebi Nadhira

*Department of Engineering Physics
Institut Teknologi Bandung
Bandung, Indonesia
vebi.nadhira@gmail.com*

Abstract—This paper proposes a coordination scheme for multiple unmanned aerial vehicle (multi-UAV) in tracking and monitoring multiple moving vessel objects in maritime patrol operations. In the proposed method, each UAV is assumed to have optical sensors which can measure its distances to moving target vessels. These measurements are processed to obtain estimates of the targets' positions, which then subsequently used to construct convex hulls that cover all detected targets. The multi-UAV tracker system then generates spatio-temporal path curves using cycloid-type trajectories with a formation geometry that is adapted to the convex hulls of the target vessels. A distributed extended Kalman filter which combines state estimates from different trackers is also used to improve the estimation accuracy of the target positions. A distributed control law is proposed to maintain the tracker-target's relative geometry which capture accurate tracking of moving target vessels. Simulation results are presented to illustrate the proposed schemes' effective performance.

Index Terms—range-based target localization, target pursuit, multi-tracker, multi-target, moving path following

I. INTRODUCTION

In recent years, unmanned aerial vehicles (UAVs) have been developed and used to perform the track and pursuit of moving targets [1]–[3]. UAVs' deployment methods have been proven to be more efficient than conventional human-led patrol approaches [4]–[6]. One of such methods is the range-based simultaneous localization and pursuit (SLAP) technique for estimating the motions of a moving target (such as car or vessel) using range data from sensors [7]–[9]. In this technique, each tracker is equipped with optical sensors and autonomous navigation systems which allow it monitors and tracks a detected moving target. When extended to the case of tracking multiple targets using multiple trackers, this technique has the potential to be implemented on multi-UAV operation for continuous and adaptive surveillance of illegal vessel/fishing activities over vast maritime areas.

This paper proposes a multi-UAV coordination approach which equips a multi-tracker SLAP with a scheme for tracking moving geometric shapes formed by the locations of multiple

moving vessels. In the proposed method, each UAV uses optical sensors to measure its distances to moving target vessels. These measurements are processed to obtain estimates of the targets' positions, which then used to construct convex hulls that cover all detected targets. The multi-UAV tracker system then generates spatio-temporal (S-T) curve paths as cycloid-type trajectories with a formation geometry that is adapted to the constructed convex hulls of the moving target vessels [10]. A distributed extended Kalman filter (DEKF) which combines state estimates from different trackers is also used to improve the estimation accuracy of all tracker vessels' positions [11]. Distributed control laws are finally designed to maintain the tracker-target's relative geometry, which ensure accurate tracking of moving target vessels.

The remainder of the paper is structured as follows. Section II describes the modeling and control problem of the multi-UAV system. Section III presents the proposed multi-UAV coordination scheme. Simulation results are given in Section IV, and the paper is concluded with remarks in Section V.

II. SYSTEM DESCRIPTION AND MODELING

A. Tracker UAV Model

Consider N UAV trackers with index $[i]$ for $i = 1, \dots, N$. Let $\{\mathcal{I}\}$ be an inertial frame for the kinematics motion of each UAV with a body frame $\{\mathcal{B}\}^{[i]}$. Let $\mathbf{p}_1^{[i]} = [p_x^{[i]}, p_y^{[i]}, p_z^{[i]}]^T$ be the UAV position vector and $\mathbf{p}_2^{[i]} = [\phi^{[i]}, \theta^{[i]}, \psi^{[i]}]^T$ be its attitude vector consisting roll ($\phi^{[i]}$), pitch ($\theta^{[i]}$), and yaw ($\psi^{[i]}$) angles with respect to (wrt) $\{\mathcal{I}\}$ (cf. Fig. 1). The state variables of each tracker is defined by $\mathbf{p}^{[i]} = [\mathbf{p}_1^{[i]}, \mathbf{p}_2^{[i]}]^T$. Let $\mathbf{u}_1^{[i]} = [v_x^{[i]}]^T$ be the surge velocity vector and $\mathbf{u}_2^{[i]} = [p^{[i]}, q^{[i]}, r^{[i]}]^T$ be the attitude velocity vector on $\{\mathcal{B}\}^{[i]}$. The input vector of tracker $[i]$ is defined as $\mathbf{u}^{[i]} \equiv [\mathbf{u}_1^{[i]}, \mathbf{u}_2^{[i]}]^T$.

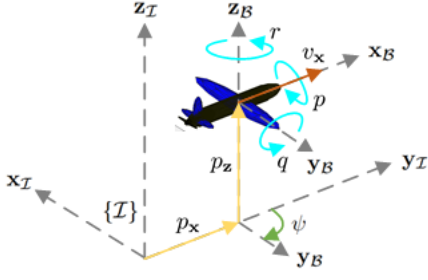


Fig. 1. The configuration of each tracker UAV in the inertial frame $\{I\}$.

The kinematics of each UAV tracker may then be expressed as follows (note that superscripts $[i]$ omitted for clarity).

$$\begin{bmatrix} \dot{p}_x \\ \dot{p}_y \\ \dot{p}_z \\ \dot{\phi} \\ \dot{\theta} \\ \dot{\psi} \end{bmatrix} = \mathbf{0}_{6 \times 6} \begin{bmatrix} p_x \\ p_y \\ p_z \\ \phi \\ \theta \\ \psi \end{bmatrix} + \begin{bmatrix} c_\psi c_\theta & 0 & 0 & 0 \\ s_\psi c_\theta & 0 & 0 & 0 \\ s_\theta & 0 & 0 & 0 \\ 0 & 1 & s_\phi t_\theta & c_\phi t_\theta \\ 0 & 0 & c_\phi & -s_\phi \\ 0 & 0 & s_\phi/c_\theta & c_\phi/c_\theta \end{bmatrix} \begin{bmatrix} v_x \\ p \\ q \\ r \end{bmatrix} \quad (1)$$

where $s_\phi = \sin(\phi)$, $c_\phi = \cos(\phi)$, and $t_\phi = \tan(\phi)$.

B. Target Vessel Model

Let there be M target vessels with index $[j]$. Let $\mathbf{q}_1^{[j]}(t) = [q_x^{[j]}, q_y^{[j]}, q_z^{[j]}]^T$ be target $[j]$'s position vector and $\mathbf{q}_2^{[j]}(t) = \dot{\mathbf{q}}_1^{[j]}(t)$ be its velocity wrt $\{I\}$. Assume the target motions can be approximated as particles with quasi-steady model (2).

$$\dot{\mathbf{q}}^{[j]}(t) = A\mathbf{q}^{[j]}(t) + \mathbf{w}(t), \quad (2)$$

where $\mathbf{q}^{[j]}(t) = [\mathbf{q}_1^{[j]}(t); \mathbf{q}_2^{[j]}(t)]$ is the target's state variables whose $\mathbf{q}_2(t)$ component is corrupted by Gaussian noise $\mathbf{w} \sim \mathcal{N}(\mathbf{0}, Q_t)$, and $A = \text{row}\{\mathbf{0}_3, \mathbf{I}_3, [\mathbf{0}_3, \mathbf{0}_3]\}$ with $\mathbf{0}_3$ and \mathbf{I}_3 are (3×3) zero and identity matrices, respectively.

C. Range Measurement Model

Let $d_k^{[i][j]}$ be the range/distance from tracker $[i]$ to target $[j]$ at discrete time k as formulated below.

$$d_k^{[i][j]} = \|\mathbf{p}_{1k}^{[i]} - \mathbf{q}_{1k}^{[j]}\|, \quad (3)$$

The tracker's noisy measurement is thus assumed to satisfy

$$y_k^{[i][j]} = \|\mathbf{p}_{1k}^{[i]} - \mathbf{q}_{1k}^{[j]}\| + \mathbf{w}_k, \quad \mathbf{w}_k \sim \mathcal{N}(0, \sigma) \quad (4)$$

Based on (3), the multi-agent tracker-target control problem can be formulated into two sub problems, namely the cooperative localization problem and cooperative pursuit problem. On one hand, the objective in cooperative localization problem is to ensure that the estimate $\hat{\mathbf{q}}^{[i][j]}$ of the target's state variables converge to a consensus among all trackers, i.e.:

$$\lim_{k \rightarrow \infty} \|\hat{\mathbf{q}}_k^{[i][j]} - \mathbf{q}_k^{[j]}\| \leq r_e. \quad (5)$$

On the other hand, the objective in cooperative pursuit problem is to ensure that over time, all trackers converge to and remain within a specified distance from the target, i.e.:

$$\lim_{t \rightarrow \infty} \|\mathbf{p}_1^{[i]}(t) - \mathbf{q}_1^{[j]}(t)\| \leq r_c. \quad (6)$$

In (5)-(6), r_c and r_e are some specified positive constants.

III. MULTI-TARGET TRACKING CONTROL SCHEME

A. Cooperative Localization

This paper uses distributed extended Kalman filter (DEKF) to address the cooperative localization task in (5) [11]. The used DEKF consists of three phases, namely *correction*, *fusion*, and *prediction*. The *correction* phase uses new measurement to update the state estimate and covariance matrix. In the *fusion* phase, each tracker's local probability density functions (PDFs) is updated based on information of its neighbors' PDFs. The *prediction* phase estimates each agent's future PDF which will be corrected at each measurement updates.

Algorithm 1 summarizes the used DEKF for estimating the states $\hat{\mathbf{q}}^{[i][j]}$ of moving target vessel j . Here, $C_k^{[i][j]}$ is the Jacobian matrix of the range measurement model, while P is an error covariance matrix which defines the information

Algorithm 1 Distributed EKF for Tracker $[i]$

```

1: procedure INITIALIZATION
2:   At  $k = 0$ , initialize  $\hat{\mathbf{q}}_{1|0}$ ,  $P_{1|0}$ 
3:    $\Omega_{1|0} = P_{1|0}^{-1}$ ,  $\mathbf{z}_{1|0} = P_{1|0}^{-1} \hat{\mathbf{q}}_{1|0}$ 
4:   return  $\hat{\mathbf{q}}_{1|0}$ ,  $\Omega_{1|0}$ ,  $\mathbf{z}_{1|0}$ 

   At each  $k$ , repeat the following procedures:
5: procedure CORRECTION
6:   if new range data is obtained then
7:      $C_k^{[i][j]} = \frac{\partial d_k^{[i][j]}}{\partial \mathbf{q}}(\hat{\mathbf{q}}_{k|k-1}^{[i][j]})$ 
8:      $\tilde{y}_k^{[i][j]} = y_k^{[i][j]} - d_k(\hat{\mathbf{q}}_{k|k-1}^{[i][j]}) + C_k^{[i][j]} \hat{\mathbf{q}}_{k|k-1}^{[i][j]}$ 
9:      $\tilde{\mathbf{z}}_k^{[i][j]} = \mathbf{z}_{k|k-1}^{[i][j]} + (C_k^{[i][j]})^\top V^{[i][j]} \tilde{y}_k^{[i][j]}$ 
10:     $\tilde{\Omega}_k^{[i][j]} = \Omega_{k|k-1}^{[i][j]} + (C_k^{[i][j]})^\top V^{[i][j]} C_k^{[i][j]}$ 
11:    else  $\tilde{\mathbf{z}}_k^{[i][j]} = \mathbf{z}_{k|k-1}^{[i][j]}$ ,  $\tilde{\Omega}_k^{[i][j]} = \Omega_{k|k-1}^{[i][j]}$ 
12: procedure COMMUNICATION
13:   Transmit  $\mathcal{M}_e(k)$  below to neighbors
14:    $\mathcal{M}_e(k) \triangleq \{\tilde{\mathbf{z}}_k^{[i][j]}, \tilde{\Omega}_k^{[i][j]}\}$ 

14: procedure FUSION (CONSENSUS ESTIMATION)
15:    $\mathbf{z}_{k|k}^{[i][j]} = \sum_{n \in \mathcal{N}_{in}^{[i]} \cup \{i\}} \pi^{[i,n]} \tilde{\mathbf{z}}_k^{[n][j]}$ 
16:    $\Omega_{k|k}^{[i][j]} = \sum_{n \in \mathcal{N}_{in}^{[i]} \cup \{i\}} \pi^{[i,n]} \tilde{\Omega}_k^{[n][j]}$ 
17:   return  $\mathbf{z}_{k|k}$ ,  $\Omega_{k|k}$ ,  $\hat{\mathbf{q}}_{k|k} = \Omega_{k|k}^{-1} \mathbf{z}_{k|k}$ 

18: procedure PREDICTION
19:    $\hat{\mathbf{q}}_{k+1|k}^{[i][j]} = F \hat{\mathbf{q}}_{k|k}^{[i][j]}$ 
20:    $\Omega_{k+1|k}^{[i][j]} = W - W F (\Omega_{k|k}^{[i][j]} + F^\top W F)^{-1} F^\top W$ 
21:   return  $\hat{\mathbf{q}}_{k+1|k}$ ,  $\Omega_{k+1|k}$ ,  $\mathbf{z}_{k+1|k} = \Omega_{k+1|k} \hat{\mathbf{q}}_{k+1|k}$ 

```

matrix $\Omega = P^{-1}$. The information vector \mathbf{z} is related to the state estimate by $\mathbf{z} = \Omega \hat{\mathbf{q}}$, where $\hat{\mathbf{q}}$ is the current state estimate. V is the measurement noise covariance matrix while $\pi^{[i,n]}$ is a weighting factor that combines state estimates of all trackers.

B. Trajectory Tracking Architecture

This paper addresses the multiple targets tracking problem using time-varying geometric shapes which capture the area enclosed by the targets' position coordinates. Such shapes are defined as convex hulls of the targets' position coordinates as they move over time, see Fig. 2. We use the centroid of the targets' convex hull as the focal coordinate of the trackers' trajectories while also optimizing the available information to enhance the targets' state estimates. The convex hull is given by $\bar{\mathbf{q}}$ with unit vector \mathbf{n} of its element of the form

$$\bar{\mathbf{q}}_n = \frac{1}{M} \sum_{j \in \mathbb{N}_j^M} q_n^{[j]} \quad (7)$$

The radius of the circular trajectory is set to be time-varying and adjusted based on the varying distance between targets and focal point. This is done while maintaining a fixed distance outside the farthest target from the centroid, α , which ensures that all targets remain inside the tracker's trajectory (cf. Fig. 2). Formally, the radius of the trackers' trajectory satisfies (8).

$$r = \max \left(\left\| \bar{\mathbf{q}}_1 - \mathbf{q}_1^{[j]} \right\| \right) + \alpha \quad (8)$$

This paper consider planar circular-shape reference trajectories for the tracker which encircle the centroid of the estimated

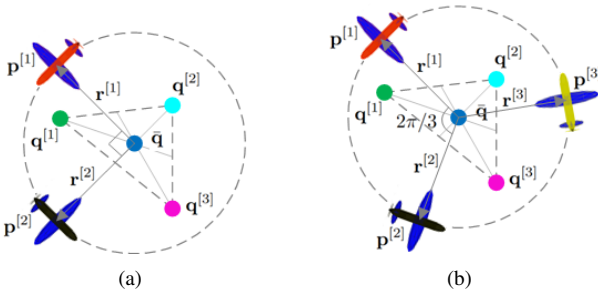


Fig. 2. Examples of tracker-target geometries: (a) 2 targets, (b) 3 targets.

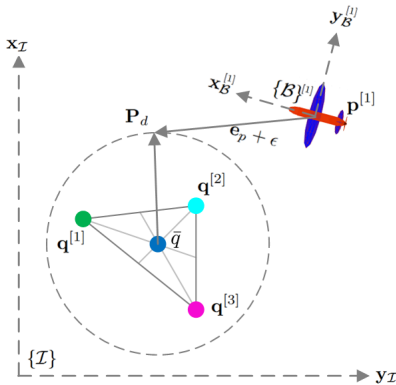


Fig. 3. Target pursuit methodology in 2D.

target positions (cf. Fig. 3). Let $\mathbf{r}(\gamma)$ be a path in inertial frame $\{\mathcal{I}\}$ with cycloid-type trajectories of the form

$$\mathbf{r}(\gamma^{[i]}) = \left[r \cos(\gamma^{[i]} + \gamma_0^{[i]}), r \sin(\gamma^{[i]} + \gamma_0^{[i]}), r_z \right]^\top \quad (9)$$

with r_z denotes the height of the trajectory as measured from the target's position and $\gamma^{[i]}$ is the path angle parameter for \mathbf{r} . Using method proposed in [12], a reference spatio-temporal (S-T) curve \mathbf{p}_d along the path around the centroid of estimated target position $\bar{\mathbf{q}}_1^{[i]}$ can be constructed as follows.

$$\mathbf{p}_d^{[i]}(\gamma^{[i]}, t) = \mathbf{r}(\gamma^{[i]}) + \bar{\mathbf{q}}_1^{[i]}(t) \quad (10)$$

For multi-tracker scenarios, the paths \mathbf{r} can be parameterized so as to ensure that the S-T curves produce the desired geometric formations relative to the target. Specifically, the parameterization is done such that $\gamma_0^{[1]} - \gamma_0^{[2]} = \pi/2$ for $N = 2$ and $\gamma_0^{[i_1]} - \gamma_0^{[i_2]} = 2\pi/N$ for $N \geq 3$, where i_1 and i_2 denote any two adjacent trackers [13].

C. Cooperative Pursuit

The cooperative pursuit task is used to ensure the tracking of moving targets and achieve the objective in (6). For this purpose, the following distributed control law for the correction speed v_c can be used as a consensus protocol.

$$v_c^{[i]} = -k_c \sum_{n \in \mathcal{N}_{in}^{[i]}} (\gamma^{[i]} - \gamma^{[n]}) \quad (11)$$

where $k_c > 0$ is a coupling gain. Using (11), the desired speed ω_d for tracking path angle parameter $\gamma^{[i]}$ can be computed as

$$\omega_d^{[i]} = \bar{\omega} + v_c^{[i]} \quad (12)$$

where $\bar{\omega}$ denotes the desired speed for all $\gamma^{[i]}$. The error in the value of γ may then be defined as follows.

$$e_\gamma^{[i]} = \dot{\gamma}^{[i]} - \omega_d^{[i]} \quad (13)$$

Taking the time derivative of (13), the dynamics of γ becomes

$$\ddot{\gamma}^{[i]} = -k_\gamma e_\gamma^{[i]} + \left(\hat{\mathbf{e}}_p^{[i]} \right)^\top R^\top \left(\mathbf{p}_2^{[i]} \right) \mathbf{r}'(\gamma^{[i]}) + \dot{v}_c^{[i]} \quad (14)$$

where $R^{[i]} \left(\mathbf{p}_2^{[i]} \right)$ is the rotation matrix for $\{\mathcal{B}\}^{[i]}$ to $\{\mathcal{I}\}$.

Define the pursuit position error \mathbf{e}_p in the tracker's body frame $\{\mathcal{B}\}^{[i]}$ to be the difference between the tracker's position and the desired trajectory. Then \mathbf{e}_p can be formulated as

$$\hat{\mathbf{e}}_p^{[i]} = R^\top \left(\mathbf{p}_2^{[i]} \right) \left(\mathbf{p}_1^{[i]} - \mathbf{r}(\gamma^{[i]}) - \bar{\mathbf{q}}_1^{[i]} \right) - \epsilon \quad (15)$$

where ϵ is an arbitrarily small non-zero vector which triggers the tracker to move towards the reference circular trajectory and thereby achieves the objective in (6). Building upon the work of [14], we derive two tracking controllers which enable the trackers to both pursue and encircle the target, which is the tracker input and γ dynamics. The tracker input \mathbf{u} is defined in (16) and is used to drive the error \mathbf{e}_p to zero.

$$\mathbf{u}^{[i]} = \bar{\Delta} \left(R^\top \left(\mathbf{p}_2^{[i]} \right) \left(\mathbf{r}'(\gamma^{[i]}) \omega_d^{[i]} + \bar{\mathbf{q}}_1^{[i]} \right) - K_p \hat{\mathbf{e}}_p^{[i]} \right) \quad (16)$$

where K_p is positive definite matrix and $\bar{\Delta} = \Delta^\top (\Delta \Delta^\top)^{-1}$, in which Δ is defined as follows.

$$\Delta = \begin{bmatrix} 1 & 0 & -\epsilon_3 & \epsilon_2 \\ 0 & \epsilon_3 & 0 & -\epsilon_1 \\ 0 & -\epsilon_2 & \epsilon_1 & 0 \end{bmatrix} \quad (17)$$

IV. SIMULATION EXPERIMENTS

This section presents the results of simulation experiments that were used to evaluate the performance of the proposed multi-UAV formation scheme for tracking three moving targets. The targets are set to follow predefined trajectories, and then two motion scenarios were considered: (i) synchronized motion, where all targets move in coordinated patterns, and (ii) spreading motion, where targets gradually diverge in different directions. The simulations were conducted using single, dual, and triple trackers to evaluate whether increasing the number of trackers improves estimation accuracy.

A. Simulation Setup

All trackers were described using kinematic model in (1) and assumed to have identical parameters. Each tracker was initialized with fixed positions and path angles. Additionally, the DEKF of each tracker is set to have similar initial state estimates and covariance matrices for each target. The trackers were set to have initial positions, orientations, trajectories, and state estimates as follows: $\mathbf{p}_0^{[1]} = [55, -60, 25, \pi, 0, 0]^T$, $\mathbf{p}_0^{[2]} = [80, 35, -50, -\frac{\pi}{4}, 0, \frac{\pi}{2}]^T$, $\mathbf{p}_0^{[3]} = [-70, 75, -4, 0, 0, 0]^T$, $\gamma_0^{[1]} = 5.49$, $\gamma_0^{[2]} = 4.71$, $\hat{\mathbf{q}}_0^{[1][i]} = [5, 0, 0, 0.2, 0.2, -0.1]^T$, $\hat{\mathbf{q}}_0^{[2][i]} = [15, 10, 0, 0.2, 0.2, -0.1]^T$, $\hat{\mathbf{q}}_0^{[3][i]} = [-10, 15, 0, 0.2, 0.2, -0.1]^T$, $\gamma_0^{[3]} = 4$, and $\hat{P}_0^{[i][j]} = \text{diag}\{[100, 100, 100, 1, 1, 0.1]^T\}$.

The control gains used in simulations are: $\epsilon = [-1, -1, 0]^T$, $\bar{\omega} = 0.1$, $u_{\min}^{[i]} = [0, -1, -1, -1]^T$, $\sigma = 10$, $u_{\max}^{[i]} = [10, 1, 1, 1]^T$, and $r_z = 20$. Simulations were conducted over a total duration of 200 seconds, with a sampling interval of 0.1 seconds and sensor measurement interval of 2 seconds.

1) *Synchronized targets Case*: For this case, all targets follow predefined trajectories while maintaining a relative formation shape. The target positions are defined as follows.

$$\begin{aligned} \mathbf{q}_1^{[1]}(t) &= [30s(0.01t), 0.1t, 0]^T \\ \mathbf{q}_1^{[2]}(t) &= [30s(0.01t) + 10, 0.1t + 10, 0]^T \\ \mathbf{q}_1^{[3]}(t) &= [30s(0.01t) - 10, 0.1t + 10, 0]^T \end{aligned} \quad (18)$$

2) *Spreading targets Case*: For this case, each target follows a distinct trajectory and diverge from each other over time. The target positions are defined as follows.

$$\begin{aligned} \mathbf{q}_1^{[1]}(t) &= [30s(0.01t), -0.1t, 0]^T \\ \mathbf{q}_1^{[2]}(t) &= [20s(0.01t) + 10, 0.15t + 10, 0]^T \\ \mathbf{q}_1^{[3]}(t) &= [-30s(0.01t) - 10, 0.1t + 10, 0]^T \end{aligned} \quad (19)$$

B. Simulation Results

Fig. 4 plots the input signals for the dual trackers with spreading targets. The figure demonstrate that as the expansion of the target path r increases, the speed of the trackers rises, potentially reaching a maximum speed limit. This underscores that the UAV has limitations on the inter-target distance, as the trackers may struggle to maintain formation accuracy when targets spread too far apart. The average estimation errors for tracking three moving targets using single, double, and triple trackers in synchronized and spreading motions are shown in Fig. 5 and Fig. 6, respectively. Additionally, using dual and triple tracker configurations significantly reduces average

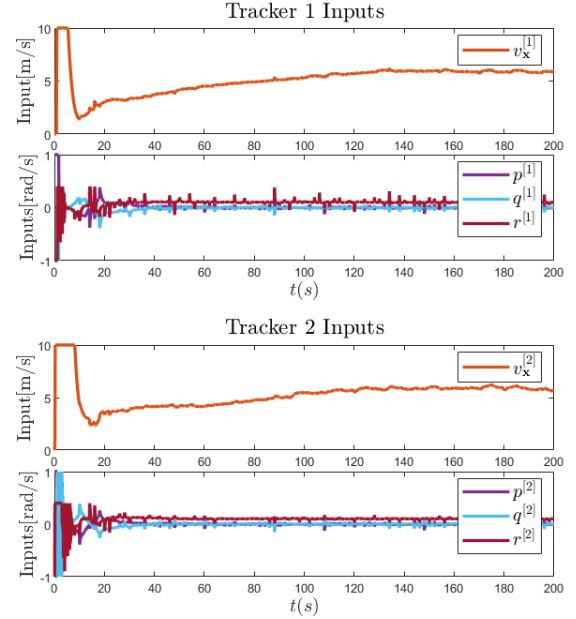


Fig. 4. Tracker's input for spreading targets dual trackers.

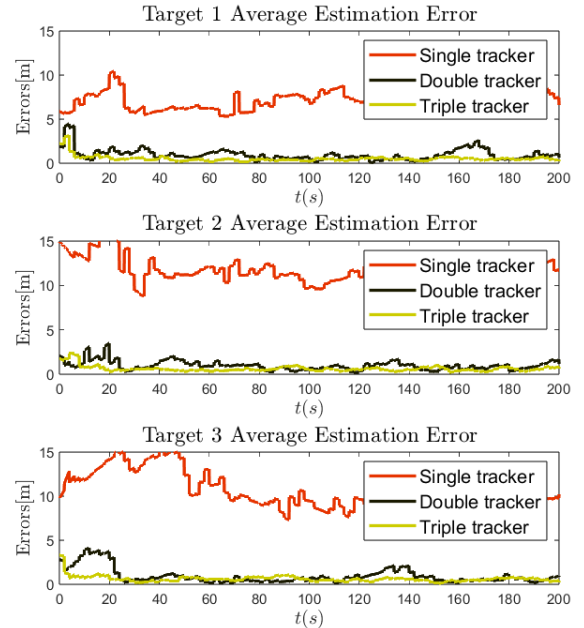


Fig. 5. Average estimation errors of synchronized target motion.

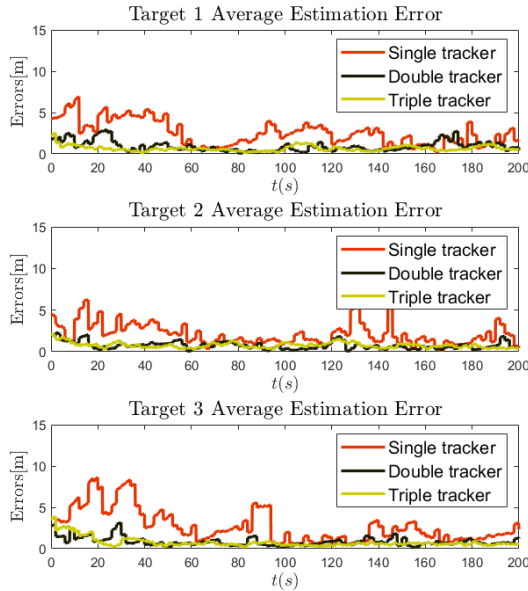


Fig. 6. Average estimation errors of spreading target motion.

estimation errors compared to a single tracker, with the triple tracker showing only a slight improvement over the dual tracker. The results further suggest a balance between the accuracy gains from additional trackers and the computational or control complexity they introduce. While triple trackers provide superior estimation accuracy, careful consideration must be given to practical constraints such as speed limits and resource allocation when scaling up the number of trackers in real-world implementations.

V. CONCLUDING REMARK

This paper has presented a multi-UAV coordination scheme for tracking control of multiple moving target objects to improve maritime surveillance/tracking of illegal fishing vessels. The proposed scheme uses range-based DEKF to estimate the target state. The integration of S-T curves and adaptive geometric formations ensures the targets remain within the sensor's measurement range at all times. This approach potentially reduces the need for extensive human resources while providing real-time tracking of illegal fishing activities.

ACKNOWLEDGMENT

This work was supported by Ministry of Education, Culture, Research, and Technology (Kemendikbudristek) of the Republic of Indonesia through a Regular Fundamental Research grant scheme in the year of 2024.

REFERENCES

- [1] C. M. Clark *et al.*, "Tracking and following a tagged leopard shark with an autonomous underwater vehicle," *J. Field Robot.*, vol. 30, no. 3, pp. 309–322, 2013.
- [2] A. Zolich, T. A. Johansen, J. A. Alfredsen, J. Kutteneuler, and E. Erstorp, "A formation of unmanned vehicles for tracking of an acoustic fish-tag," in *Proc. OCEANS 2017-Anchorage*, 2017, pp. 1–6.
- [3] G. Bonaventura and T. A. Tamba, "Multi quadrotors coverage optimization using reinforcement learning with negotiation," *IAES Int. J. Artif. Intell.*, vol. 13, no. 3, pp. 2978–2986, 2024.
- [4] M. S. Arifin *et al.*, "Experimental modeling of a quadrotor uav using an indoor local positioning system," in *Proc. 5th Int. Conf. Electric Vehicular Technology*, 2018, pp. 25–30.
- [5] N. Crasta, D. Moreno-Salinas, B. Bayat, A. M. Pascoal, and J. Aranda, "Range-based underwater target localization using an autonomous surface vehicle: Observability analysis," in *Proc. IEEE/ION Position, Location and Navigation Symposium (PLANS)*, 2018, pp. 487–496.
- [6] Y. Y. Nazaruddin *et al.*, "Communication-efficient optimal-based control of a quadrotor uav by event-triggered mechanism," in *Proc. 5th Asian Conf. Defense Technol.*, 2018, pp. 96–101.
- [7] I. Masmitja *et al.*, "Optimal path shape for range-only underwater target localization using a wave glider," *Int. J. Robot. Res.*, vol. 37, no. 12, pp. 1447–1462, 2018.
- [8] N. Crasta, D. Moreno-Salinas, A. M. Pascoal, and J. Aranda, "Multiple autonomous surface vehicle motion planning for cooperative range-based underwater target localization," *Annu. Rev. Control*, vol. 46, pp. 326–342, 2018.
- [9] T.-M. Nguyen, Z. Qiu, M. Cao, T. H. Nguyen, and L. Xie, "An integrated localization-navigation scheme for distance-based docking of UAVs," in *Proc. IEEE/RSJ IROS*, 2018, pp. 5245–5250.
- [10] T. Oliveira, A. P. Aguiar, and P. Encarnação, "Moving path following for unmanned aerial vehicles with applications to single and multiple target tracking problems," *IEEE Trans. Robot.*, vol. 32, no. 5, pp. 1062–1078, 2016.
- [11] G. Battistelli and L. Chisci, "Stability of consensus extended Kalman filter for distributed state estimation," *Automatica*, vol. 68, pp. 169–178, 2016.
- [12] T. Oliveira, A. P. Aguiar, and P. M. M. Encarnação, "Moving path following for unmanned aerial vehicles with applications to single and multiple target tracking problems," *IEEE Trans. Robot.*, vol. 32, pp. 1062–1078, 2016.
- [13] N. T. Hung, N. Crasta, D. Moreno-Salinas, A. M. Pascoal, and T. A. Johansen, "Range-based target localization and pursuit with autonomous vehicles: An approach using posterior CRLB and model predictive control," *Robot. Auton. Syst.*, vol. 132, p. 103608, 2020.
- [14] N. T. Hung, F. F. C. Rego, and A. M. Pascoal, "Cooperative distributed estimation and control of multiple autonomous vehicles for range-based underwater target localization and pursuit," *IEEE Trans. Control Syst. Technol.*, vol. 30, no. 4, pp. 1433–1447, 2022.